ELSEVIER

Catalysis Today 78 (2003) 467–475

CATALYSIS TODAY

www.elsevier.com/locate/cattod

Characterization and catalytic evaluation of mesoporous and microporous molecular sieves containing niobium

Martin Hartmann [a,*], A.M. Prakash [b], Larry Kevan [b]

[a] *Department of Chemistry, Chemical Technology, University of Kaiserslautern, PO Box 3049, D-67653 Kaiserslautern, Germany*
[b] *Department of Chemistry, University of Houston, Houston, TX 77204-5003, USA*

Abstract

The synthesis and characterization of the novel microporous aluminophosphate NbAPO-5 is described. The novel material has been studied by X-ray powder diffraction, SEM, TG/DTA-MS, electron spin resonance, and ultraviolet-visible (UV-Vis) spectroscopy The catalytic properties have been tested in the epoxidation of 1-hexene and cyclohexene, respectively, in comparison with niobium-containing silicalite-1 and NbMCM-41. The results of the physical characterization indicate that it is possible to prepare niobium-containing aluminophosphates, where isolated Nb(V) species are connected to framework defect sites via formation of Nb–O–P or Nb–O–Al bonds. The results of this study allow the preparation of microporous and mesoporous niobium-containing molecular sieves which are active catalysts in oxidation reactions.

Keywords: Niobium; Aluminophosphate; ESR spectroscopy; Cyclohexene oxidation

1. Introduction

Synthesis of transition metal containing molecular sieves (microporous as well as mesoporous) is one of the fastest developing areas in molecular sieve science, as evidenced by recent published reviews [1,2]. Several transition metals have been substituted into crystalline silica or aluminophosphate frameworks to yield the corresponding metallosilicate or metalloaluminophosphate molecular sieves. However, the location of the metal species and their state always remain uncertain, despite the employment of numerous different characterization methods comprising IR, electron spin resonance (ESR) and ultraviolet-visible (UV-Vis) spectroscopy.

Recently, there has been a growing interest into niobium- and tantalum-containing molecular sieves [3]. The introduction of niobium into mesoporous molecular sieves has been studied by Ziolek et al. [4,5], while Antonelli and Ying [6] reported the synthesis of mesoporous niobium oxide. The synthesis and characterization of niobium- and tantalum-containing silicalite-1 (NbS-1 and TaS-1) was published recently [7–9] and some evidence has been presented for isomorphous substitution [7,9] of Nb and Ta into the silicalite-1 framework. The syntheses of NbS-2 (MEL) [10] and of a new molecular sieve named NbAM-11 have been reported as well [11]. The latter material was found to contain niobium in octahedral coordination.

Niobium and tantalum—which belong to the same group in the periodic table as vanadium (group Vb)—have shown remarkable catalytic properties. Nb_2O_5 or Ta_2O_5 as a single phase or in combination with other

* Corresponding author. Tel.: +49-631-205-3559; fax: +49-631-205-4193.
E-mail address: hartmann@rhrk.uni-kl.de (M. Hartmann).

0920-5861/02/$ – see front matter
PII: S0920-5861(02)00334-6

transition metal oxides possess interesting catalytic properties in a large number of reactions, e.g., the oxidative dehydrogenation or ammoxidation of alkanes and the dehydrogenation of alcohols [12,13]. The potential of niobium-containing molecular sieves for catalytic applications has only been scarcely addressed. NbMCM-41 was found to exhibit a high activity in the oxidation of thioethers to sulfoxides with H_2O_2 [14,15] and the formation of glycol monoethers [16]. Furthermore, NbS-1 and TaS-1 showed high activity in the (acid catalyzed) Beckmann rearrangement of cyclohexanone oxime to ε-caprolactam [17]. A recent patent describes that a niobium-containing silicalite-1 has been surprisingly found to be active as an olefin epoxidation catalyst using aqueous hydrogen peroxide [18].

In this work, we report the hydrothermal synthesis and characterization of the crystalline niobium-containing aluminophosphate NbAPO-5. Results from powder X-ray diffraction (XRD), UV-Vis, and ESR spectroscopy are discussed to investigate the incorporation of niobium into the aluminophosphate framework. The catalytic properties of this novel material are discussed in comparison to NbS-1 and NbMCM-41 using 1-hexene and cyclohexene oxidation in the liquid phase as test reactions.

2. Experimental section

2.1. Synthesis

NbAPO-5 was prepared hydrothermally using tetraethyammonium hydroxide (TEAOH) as the organic template. The following chemicals were used without further purification: orthophosphoric acid (85 wt.% in water), Disperal Sol P2 (CONDEA, 73 wt.% Al_2O_3) niobium ethoxide (Alpha, 99.999% pure) and TEAOH (Aldrich, 35 wt.% in water). Syntheses were carried out in stainless steel autoclaves lined with Teflon under autogenous pressure without agitation. The following gel composition was used for the syntheses of NbAPO-5: Al_2O_3:0–0.06 Nb_2O_5:1.1 P_2O_5:0.944 TEAOH:53 H_2O. In a typical synthesis of NbAPO-5, 6.4 g of Disperal Sol P2 were added to a solution of 11.6 g of phosphoric acid in 18.2 g of distilled water. The mixture was homogenized for 45 min and subsequently 0.4 g of $Nb(C_2H_5O)_5$ were added. After the addition of 18.2 g TEAOH, the gel was homogenized for another 45 min. Crystallization was achieved at 150 °C for 24 h.

After synthesis the materials were recovered by filtration, washed with water and finally calcined in flowing air up to 540 °C for 48 h. The syntheses of NbS-1 and NbMCM-41 and the impregnation of silicalite-1 with niobium isopropoxide are described elsewhere [8,19].

2.2. Characterization

The chemical composition of the samples was determined by inductively coupled plasma-atomic emission spectroscopy (ICP-AES). X-ray powder diffraction patterns were recorded after synthesis and template removal on a Siemens D5005 diffractometer using Cu Kα radiation. TG/DTA-MS measurements were carried out under flowing nitrogen in a high resolution thermogravimetric analyzer (SETARAM Setsys 16MS) with a heating rate of 10 K/min.

The UV-Vis spectra were recorded on a Perkin-Elmer Lamda 16 spectrometer in the diffuse reflectance mode. ESR spectra were recorded at X-band on a Bruker ESP 300 spectrometer at −196 °C. The samples were loaded into 3 mm o.d. by 2 mm i.d. Suprasil quartz tubes, which were evacuated to a final pressure of 10^{-5} kPa at 420 °C overnight. The activated samples were sealed, immersed in liquid nitrogen and finally exposed to γ-irradiation of a ^{60}Co source to a total dose of 1.1 Mrad at a dose rate of 0.18 Mrad h^{-1} before the ESR experiments.

2.3. Catalytic tests

The catalytic experiments were conducted in the liquid phase at 60 °C using 11.9 mmol of cyclohexene, 11.9 mmol of hydrogen peroxide (30 wt.% in water) and 0.2 g of catalyst in 20 cm^3 of acetonitrile as a solvent. For the epoxidation of 1-hexene (20 mmol), 11.9 mmol of *tert*. butylhydroperoxide (70 wt.% in water) and 0.2 g of catalyst in 20 cm^3 acetonitrile as a solvent were used. The catalysts were dried at 120 °C prior to their use. Small samples of 1 μl were regularly withdrawn from the reaction mixture and analyzed by capillary gas chromatography. Product analysis was achieved by GC–MS.

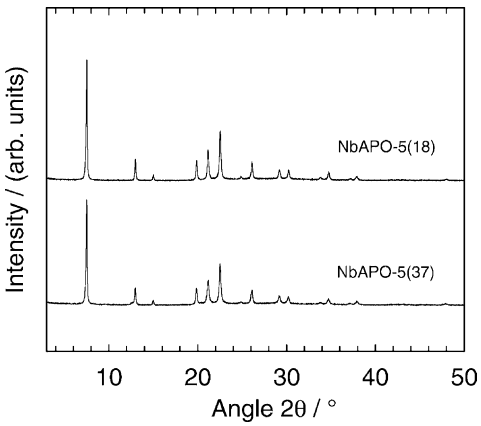

Fig. 1. XRD patterns of calcined NbAPO-5(37) and NbAPO-5(18).

3. Results and discussion

3.1. Characterization

The powder XRD patterns of calcined NbAPO-5(37) and NbAPO-5(18) are shown in Fig. 1. The observed patterns confirm the AFI-structure (structure of $AlPO_4$-5) for both samples and the absence of impurities and competing phases. The results of the chemical analysis of the calcined samples are summarized in Table 1.

SEM micrographs showed that pure NbAPO-5 exhibited the form of spherical (or occasionally diabolo-shaped) particles of up to 40 μm diameter (Fig. 2a). The particle size decreased slightly with increasing Nb content of the sample. The spherical or diabolo-shaped aggregates are formed from hexagonal platelets (Fig. 2b). Similar findings have also been reported for CoAPO-5 [20] and TAPSO-5 [21].

Table 1
Chemical analysis of selected samples

Sample	n_{Si}/n_{Nb} (gel)	n_{Si}/n_{Nb} (ICP)	n_{Al}/n_{Nb} (gel)	n_{Al}/n_{Nb} (ICP)
NbS-1(41)	60	40.7	–	–
NbS-1(88)	120	88.4	–	–
Nb/silicalite-1	40	40.0	–	–
NbAPO-5(37)	–	–	40	37.1
NbAPO-5(18)	–	–	20	17.9
NbMCM-41	64	58.2	–	–

Fig. 3 exhibits the TG, DTG and DTA curves for the calcination of NbAPO-5(37) and $AlPO_4$-5 in a nitrogen flow. For both samples three distinct stages of weight loss are observed. Between 50 and 150 °C about 3.3 wt.% of water is desorbed from $AlPO_4$-5 (endothermic process), while NbAPO-5(37) releases about 4.8 wt.% of water. The second weight loss around 290 °C is also endothermic and is ascribed to the template decomposition via a Hofmann-type degradation. The decomposition produces triethylamine as evident from the respective mass spectra. Between 340 and 400 °C, a third (endothermic) weight loss is detected, which is ascribed to the desorption of strongly adsorbed template fragments. The total amount of template desorbed from the sample is ca. 9.2 and 9.6 wt.% for NbAPO-5(37) and $AlPO_4$-5, respectively.

The UV-Vis spectra of calcined hydrated NbAPO-5(37) and NbAPO-5(18) exhibit one maximum near 200 nm and a shoulder around 240 nm (Fig. 4). A transition with two maxima near 220 and 245 nm is also reported for NbS-1 [7,8]. On the other hand, for niobia (Nb_2O_5) a very broad band with a maximum at 350 nm and an absorption onset near 450 nm is observed. In the NbAPO-5 samples, the absence of signals between 350 and 450 nm indicates that niobia-like phases were not formed. Silicalite-1 impregnated with niobium isopropoxide ($n_{Si}/n_{Nb} = 40$) and NbMCM-41 show a somewhat similar absorption band, which is broader than the spectrum of NbS-1. Nevertheless, Antonelli and Ying [6] suggest the formation of Nb–O–Si bonds in NbMCM-41. The observation of a broad UV absorption band in the spectrum of Nb_2O_5 is consistent with the known bandgap of this material (410 nm). Anpo et al. [22] have proposed that the band energy gap position shifts to higher energy with a decrease in particle size of a semiconductor material. A sharp transition between 200 and 220 nm as observed for NbAPO-5 and NbS-1, respectively, therefore suggests that it is associated with local Nb–O bonds. Tanaka et al. [23] have studied highly dispersed niobia on a silica surface using diffuse reflectance and photo-luminescence spectroscopy. For samples with low niobia loading, the UV-Vis spectra show a sharp absorption band between 200 and 330 nm with a maximum near 220 nm. In contrast, samples having a higher niobium loading show a broader absorption band between 200 and 370 nm with a maximum near 270 nm.

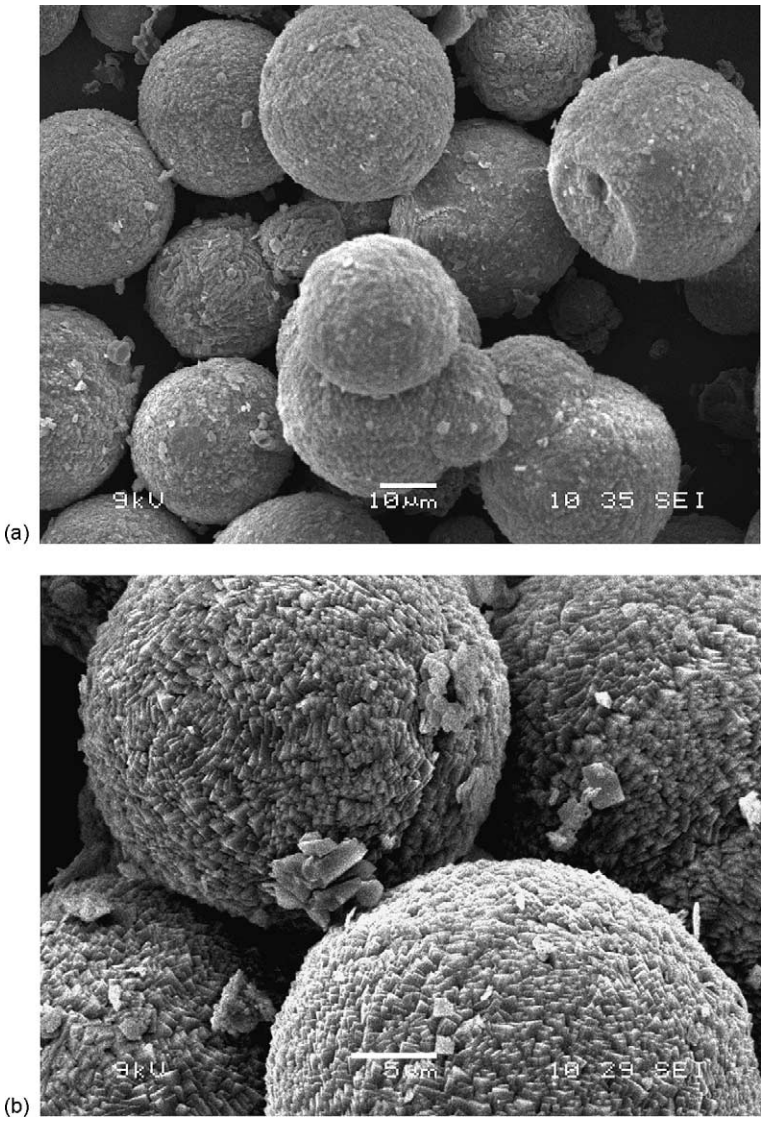

Fig. 2. Scanning electron micrographs of NbAPO-5(37).

On the basis of photo-luminescence and X-ray absorption near edge structure (XANES) results, the authors assigned the maximum at 220 nm to monomeric and oligomeric NbO_4 tetrahedra. The absorption band at 270 nm for samples with high niobium loading is assigned to microparticles of Nb_2O_5. It is generally accepted that at low niobium loadings, the dehydrated surface niobia species on silica predominantly consist of monomeric NbO_4 species. Upon hydration, however, the coordination of the coordination number of the surface niobia species may increase from 4-fold to 6-fold due to the adsorption and coordination of water molecules [24]. The spectra of hydrated NbAPO-5 (Fig. 4) and NbS-1 are similar to those reported with low niobium loading indicating monomeric NbO_4 species, while the spectra of hydrated NbMCM-41 and Nb/silicalite-1 are closer to those with high niobium loading. Recently Gao et al. [25] reported that niobium

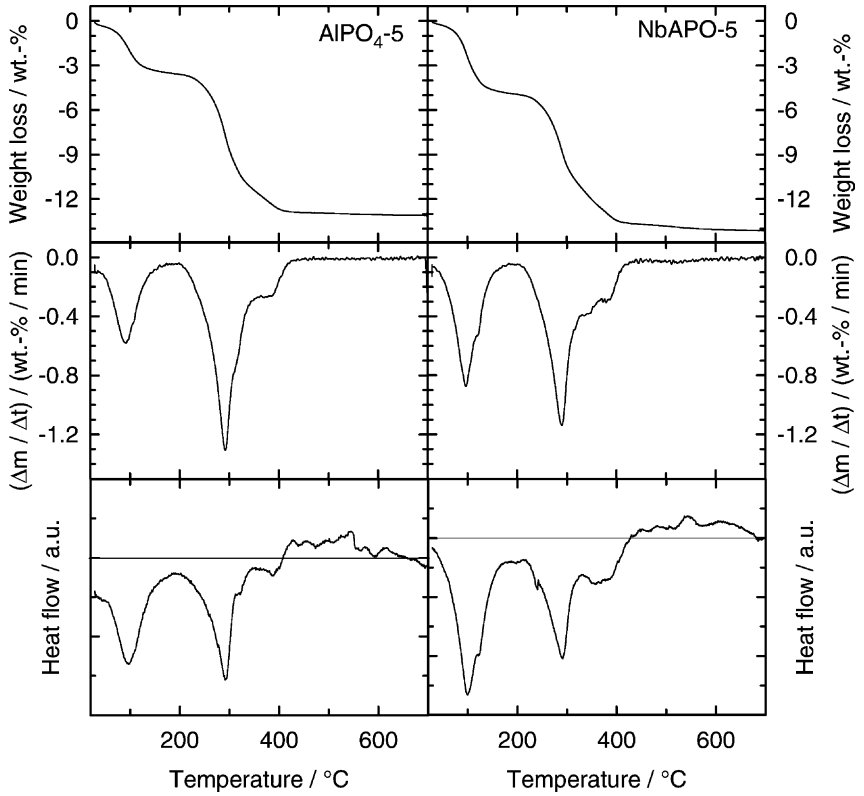

Fig. 3. TG, DTG and DTA curves of NbAPO-5(37) and $AlPO_4$-5.

in dehydrated NbMCM-41 and 1% Nb_2O_5/SiO_2 predominately exists as monomeric NbO_4 species, while monomeric surface niobia species and/or bulk Nb_2O_5 are formed on silica under hydrated condition.

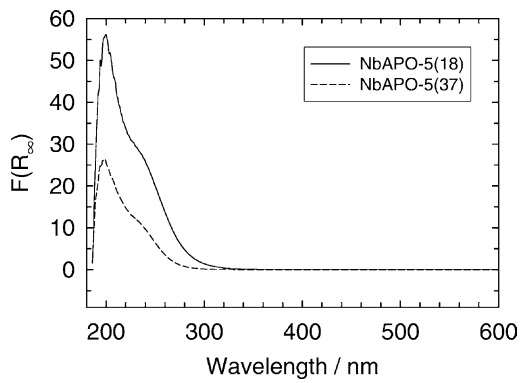

Fig. 4. UV-Vis spectra of hydrated calcined NbAPO-5 samples.

Therefore, from the UV-Vis spectra alone, unambiguous evidence for the isomorphous substitution of niobium into AFI and MFI frameworks cannot be obtained.

Fig. 5 shows the wide-field and center-field ESR spectra of activated NbAPO-5(37) after γ-irradiation at −196 °C. Calcined, dehydrated and activated samples of NbAPO-5 and the respective parent material $AlPO_4$-5 show no ESR signal at −196 °C. Under the same pretreatment conditions, pure Nb_2O_5, and Nb_2O_5 mixtures with $AlPO_4$-5 also do not show any signal. Therefore, niobium in NbAPO-5 is Nb(V), which is not paramagnetic. The γ-irradiation of dehydrated NbAPO-5, however, induces a rich ESR spectrum with multiple signals.

The intense line around $g = 2.0$ is due to radiation defect centers in the quartz tube. These are radiation-induced hole centers trapped in the lone-pair p-orbitals of the associated oxygen atoms. The

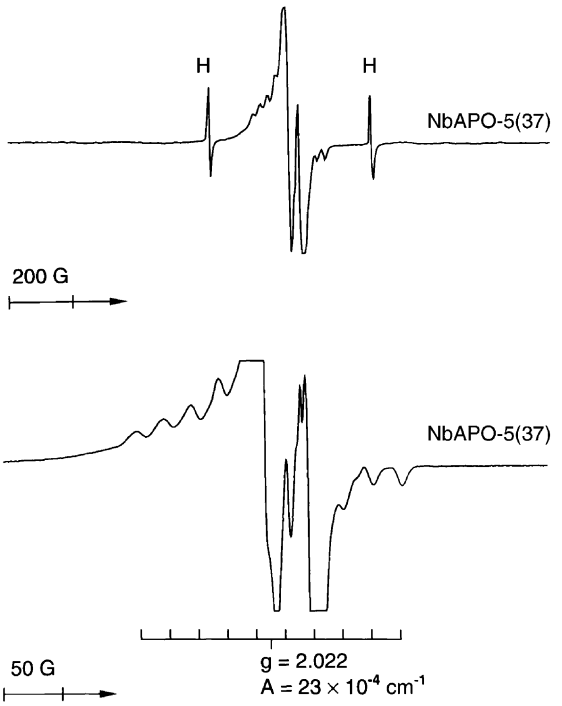

Fig. 5. ESR spectra at 77 K of NbAPO-5(37).

sharp intense lines labeled H are the characteristic ∼505 G doublet from hydrogen atoms also generated and trapped in the quartz tube during irradiation at −196 °C, which decays rather quickly. The radiation defect centers and the hydrogen atoms are also detected after irradiating a quartz tube filled with $AlPO_4$-5, so they are not associated with niobium. The remaining signal in both NbAPO-5 samples has $g_{av} = 2.022$ and a 10-line hyperfine structure with a splitting of $\sim 23 \times 10^{-4}\,cm^{-1}$ due to the interaction with the ^{93}Nb nucleus ($I = 9/2$). It should be mentioned that no ESR signal similar to this one is observed in the spectrum of pure Nb_2O_5 after γ-irradiation at −196 °C. The *g*-value of this signal is larger than the free electron *g*-value of 2.0023, which indicates that these signals are for hole centers and not electron centers. Therefore, the signal with the 10-line hyperfine structure can clearly be assigned to hole centers located on P–O–Nb or Al–O–Nb units located in the framework of NbAPO-5. This signal cannot be assigned to defects generated on Nb–O–Nb units, because one would expect more than 10 hyperfine lines for such a case and this signal was not observed for a mixture of Nb_2O_5 with $AlPO_4$-5. An analogous signal, however, is observed in Nb_2O_5–Na_2O–SiO_2 glasses [26] and NbS-1 [7] after γ-irradiation.

In contrast to our results for dehydrated NbS-1 and NbMCM-41 [7,19], an underlying broad spectrum (characteristic for Nb(IV)) is not observed for dehydrated NbAPO-5. Such a signal was assigned to Nb(IV) ions in isolated NbO_4 units, which are formed by radiolytic reduction of Nb(V) and exhibit an axially symmetric ESR signal with a 10-line hyperfine structure [7,19].

The presented results suggest that it is possible to prepare niobium-containing NbAPO-5, in which isolated NbO_4 species are located in the aluminophosphate framework. However, these species are Nb(V) and we tentatively assume that they are replacing phosphorous in the original $AlPO_4$ framework [27]. Furthermore in contrast to our results on NbS-1 and NbMCM-41 [7,19], reduction of Nb(V) to Nb(IV) by γ-irradiation failed. We, therefore, conclude that the mechanism of isomorphous substitution of niobium into zeolites and aluminophosphates is distinctly different.

3.2. Catalytic results

The potential of niobium-containing molecular sieves for catalytic applications has only been scarcely addressed. We have, therefore, tested NbAPO-5 in comparison to NbS-1 and NbMCM-41 in the oxidation of 1-hexene and cyclohexene. None of the aforementioned catalysts showed any activity in the epoxidation of 1-hexene. In the Arco patent [18], however, a significant catalytic activity of NbS-1 for 1-hexene oxidation was claimed. The activity of the described NbS-1 catalyst increases significantly, when the catalyst was stirred for 24 h in H_2O_2 prior to the reaction, which indicates that leaching of niobium into the reaction mixture has to be considered. In fact, we observed a 1-hexene conversion of 24% (after 24 h of reaction) for a Nb/silicalite-1 sample, which was prepared by impregnation of silicalite-1 with niobium isopropoxide [8].

In Figs. 6 and 7, the results of cyclohexene oxidation over different niobium-containing catalysts are depicted. For silicalite 1 (and the other parent materials $AlPO_4$-5 and MCM-41) and NbAPO-5 yields of

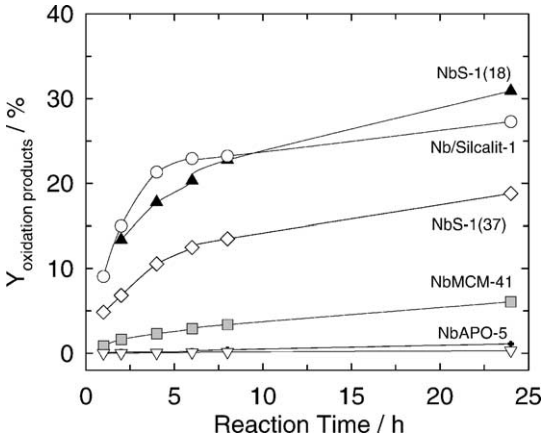

Fig. 6. Yield of oxidation products obtained over different niobium-containing catalysts (the reaction conditions are described in the experimental section).

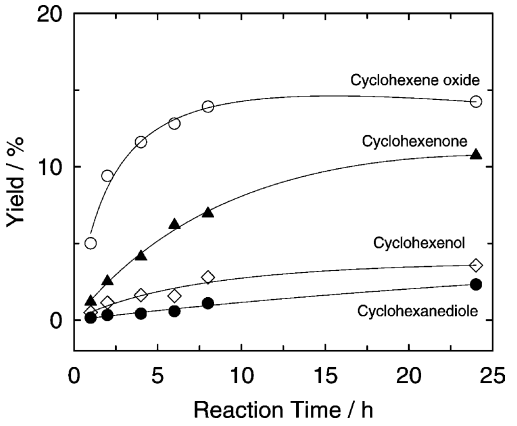

Fig. 7. Oxidation of cyclohexene with H_2O_2 over NbS-1(41).

oxidation products below 1% are observed after a reaction time of 24 h. For NbS-1(88) the product yield reaches 14% after 24 h, while for the catalyst with the higher niobium loading (NbS-1(41)) also the product yield increased by a factor of 2. A comparable product yield was observed for the impregnated sample Nb/silicalite-1. After a reaction time of 4–5 h, the reaction slows down considerably over some catalysts under investigation. This indicates that the catalytic system is probably poisoned by strong adsorption of polar products. The primary oxidation product over NbS-1(41) is cyclohexene oxide, which is converted to cyclohexane diole only to a minor extent. The formation of 1,2-cyclohexane-dione and adipic acid is not observed. Additionally, large amounts of cyclohexenone and cyclohexenol, which are the result of an allylic oxidation, are observed [28]. The yields of the different oxidation products obtained for all catalysts under investigation are summarized in Table 2.

The conversion of cyclohexene observed over NbS-1 in the present study is significantly higher as compared to titanium-containing silicalite-1 (TS-1). In particular, Corma et al. [29] and Tuel [21] reported that cyclohexene was not or only to a small extent (X_{C-H_x} = 1.7% (6 h)) oxidized over TS-1. They concluded that the pores of the MFI structure are too small and the formation of the epoxide is sterically hindered. In contrast, the epoxidation of cyclohexene is observed over VAPO-5 [30] and TAPSO-5 [21], while NbAPO-5 exhibited no activity in the present study independently of the oxidizing agent (H_2O_2 or *tert*-butyl-hydroperoxide) employed. One possible explanation for this apparent contradiction is that niobium is leached into the reaction mixture from the

Table 2
Niobium-catalyzed oxidation of cyclohexene with H_2O_2 (T_R = 60 °C, m_{cat} = 200 mg, reaction time 4 h)

Catalyst	$X_{cyclohexene}$ (%)	$Y_{cyclohexene\ oxide}$ (%)	$Y_{cyclohexane\ diole}$ (%)	$Y_{cyclohexenol}$ (%)	$Y_{cyclohexenone}$ (%)
Silicalite-1	0.1	0	0	0	0.1
NbS-1 (88)	11	7.1	0.3	0.8	2.3
NbS-1 (41)	18	11.6	0.4	1.6	4.1
Nb/silicalite-1	22	17.7	0.7	1.2	2.2
MCM-41	0.5	0.4	0	0	0.1
NbMCM-41(64)	3	0.4	0.4	0.3	1.2
$AlPO_4$-5	0.2	0.01	0	0.03	0.2
NbAPO-5(37)	0.1	0.02	0	0.04	0.1
NbAPO-5(18)	0.2	0.05	0	0.02	0.1

NbS-1 catalysts and homogeneous catalysis occurs. However, only little activity of the remaining solution was found after hot filtration of the catalyst from the reaction mixture, which is typically considered evidence for true heterogeneous catalysis. In contrast, the impregnated sample Nb/silicalite was active in both reactions, the epoxidation of 1-hexene and cyclohexene, which supports an argument in favor of niobium leaching. For NbAPO-5 we assume true isomorphous substitution into the aluminophosphate framework. This catalyst is not active in the oxidation of cyclohexene under our reaction conditions, which excludes leaching of niobium and is in line with our ESR experiments, where reduction of Nb(V) to Nb(IV) was not observed even after γ-irradiation. However, the superior activity of NbS-1 as compared to NbAPO-5 could also be due to the fact that Nb–O–Si bonds are significantly more reducible and redox active than the stable Nb–O–Al and Nb–O–P bonds [31,32]. This could also account for the differences in ESR spectra of NbS-1 and NbAPO-5 observed after γ-irradiation, which shows that reduction Nb(V) to Nb(IV) is more difficult in the latter material.

4. Conclusions

We have shown that it is possible to incorporate niobium into aluminophosphate materials by direct synthesis. The results indicated that Nb(V) is well dispersed in the $AlPO_4$ framework. After γ-irradiation of the activated niobium molecular sieves radiation-induced hole centers (V centers) located on Al–O–Nb or P–O–Nb units are observed. In contrast to the results obtained with NbS-1 and NbMCM-41, reduction of Nb(V) to Nb(IV) was not achieved, which limits the use of these materials in oxidation reactions.

However, NbS-1 and NbMCM-41 are found to be active in the oxidation of cyclohexene, but no activity for the epoxidation of 1-hexene was detected. The activity of NbS-1 is comparable to a Nb/silicalite-1 catalyst prepared by impregnation of silicalite-1 with niobium isopropoxide. Based on our results, we have to assume that (at least part of) the observed activity is due to niobium leaching into the reaction mixture, but differences in the reducibility and redox activity of Nb–O–Si and Nb–O–Al (Nb–O–P) bonds have also to be considered. This is in line with our ESR results showing that reduction of Nb(V) to Nb(IV) is more difficult in NbAPO-5 as compared to NbS-1.

Acknowledgements

Financial support from Deutsche Forschungsgemeinschaft (DFG), Fonds der Chemischen Industrie and Robert A. Welch Foundation (LK) is gratefully acknowledged. LK and MH thank the NSF and the DAAD for a travel grant.

References

[1] M. Hartmann, L. Kevan, Chem. Rev. 99 (1999) 635.
[2] A. Tuel, Micropor. Mesopor. Mater. 27 (1999) 151.
[3] I. Nowak, M. Ziolek, Chem. Rev. 99 (1999) 3603.
[4] M. Ziolek, I. Nowak, J.C. Lavalley, Catal. Lett. 45 (1997) 259.
[5] M. Ziolek, I. Nowak, Zeolites 18 (1997) 356.
[6] D.M. Antonelli, J.Y. Ying, Angew. Chem. Int. Ed. Engl. 35 (1995) 426.
[7] A.M. Prakash, L. Kevan, J. Am. Chem. Soc. 120 (1998) 13148.
[8] M. Hartmann, Chem. Lett. (1999) 407.
[9] Y.S. Ko, W.S. Ahn, Micropor. Mesopor. Mater. 30 (1999) 283.
[10] N.B. Milestone, S. Sahasrabudhe, in: M.M. Treacy, B.K. Marcus, M.E. Bisher, J.B. Higgins (Eds.), Proceedings of the 12th International Zeolite Conference, Materials Research Society, Warrendale, PA, 1999, pp. 1901–1908.
[11] J. Rocha, P. Brandano, A. Phillippou, M.W. Anderson, Chem. Commun. (1999) 2687.
[12] G. Giu, P. Grange, J. Catal. 156 (1995) 132.
[13] O. Desponds, R.L. Keiski, G.A. Somorjai, Catal. Lett. 19 (1993) 17.
[14] M. Ziolek, I. Sobczak, P. Decyk, I. Nowak, J. Kujawa, Micropor. Mesopor. Mater. 35–36 (2000) 195.
[15] M. Ziolek, A. Lewandowska, M. Renn, I. Nowak, P. Decyck, J. Kujawa, in: A. Galarneau, F. Di Renzo, F. Fajula, J. Vedrine (Eds.), Zeolites and Mesoporous Materials at the Dawn of the 21st Century, Studies in Surface Science and Catalysis, vol. 135, Elsevier, Amsterdam, 2001, p. 27-P-09.
[16] J. Xin, J. Suo, X. Zhang, Z. Zhang, New J. Chem. 24 (2000) 569.
[17] W.S. Ahn, K.Y. Kim, M.H. Kim, Y.S. Uh, in: A. Galarneau, F. Di Renzo, F. Fajula, J. Vedrine (Eds.), Zeolites and Mesoporous Materials at the Dawn of the 21st Century, Studies in Surface Science and Catalysis, vol. 135, Elsevier, Amsterdam, 2001, p. 01-P-14.
[18] R.J. Saxton, J.G. Zajacek, US Patent 5,618,512 (1997), assigned to Arco Chemical Technology.
[19] M. Hartmann, S. Ernst, A.M. Prakash, L. Kevan, in: A. Sayari, M. Jaroniec, T.J. Pinnavaia (Eds.), Nanoporous Materials. II. Studies in Surface Science and Catalysis, vol. 129, Elsevier, Amsterdam, 2000, pp. 201–208.

[20] A.M. Prakash, K.V. Rao, S. Unnikrishnan, Ind. J. Chem. A 32 (1993) 947.
[21] A. Tuel, Zeolites 15 (1995) 228.
[22] M. Anpo, N. Aikawa, Y. Kubokawa, M. Che, C. Louis, E. Giamello, J. Phys. Chem. 89 (1985) 5017.
[23] T. Tanaka, H. Nojima, H. Yoshida, H. Nakagawa, T. Funabiki, S. Yoshida, Catal. Today 16 (1993) 297.
[24] H. Yoshida, T. Tanaka, T. Yoshida, T. Funabiki, S. Yoshida, Catal. Today 28 (1996) 79.
[25] X. Gao, I.E. Wachs, M.S. Wong, J.Y. Ying, J. Catal. 203 (2001) 18.
[26] Y.M. Kim, D.E. Rerdon, P.J. Bray, J. Chem. Phys. 48 (1968) 3396.
[27] A.M. Prakash, M. Hartmann, L. Kevan, J. Phys. Chem. B 104 (2000) 1610.
[28] P.P. Knops-Gerits, F. Thibault-Starzyk, P.A. Jacobs, in: J. Weitkamp, H.G. Karge, H. Pfeiffer, W. Hölderich (Eds.), Zeolites and Related Microporous Materials: State of the Art 1994, Studies in Surface Science and Catalysis, vol. 84, Elsevier, Amsterdam, 1994, pp. 1411–1418.
[29] A. Corma, M.A. Camblor, P. Esteve, A. Martinez, J. Perez-Pariente, J. Catal. 145 (1994) 151.
[30] M.S. Rigutto, H. van Bekkum, J. Mol. Catal. 81 (1993) 77.
[31] J.M. Jehng, I.E. Wachs, Catal. Today 8 (1990) 37.
[32] J.M. Jehng, I.E. Wachs, Catal. Today 16 (1993) 417.